Postulation of the Mechanism of the Selective Synthesis of Isotactic Poly(methyl methacrylate) Catalysed by [Zr{(Cp)(Ind)CMe_2}(Me)(thf)](BPh_4): A Hartree–Fock, MP2 and Density Functional Study**

Markus Hölscher, Helmut Keul, and Hartwig Höcker*[a]

Abstract: The bridged, C_1-symmetric, single-component zirconocene [Zr{(Cp)-(Ind)CMe_2}(Me)(thf)](BPh_4) (Ind = indenyl, Cp = cyclopentadienyl) polymerises methyl methacrylate (MMA) selectively to isotactic poly(methyl methacrylate) (PMMA) without further cocatalysts or activators. To elucidate the stereoselective steps of the polymerisation of MMA by using this catalyst we studied the propagation steps occurring with the derivative [Zr{(Cp)(Ind)CH_2}-{-O-C(OMe)=C(Me)(Et)}(MMA)]$^+$ by ab initio calculations at the Hartree–Fock(HF) level of theory. After the initiation step, which consumes the first two MMA molecules, each new catalytic cycle begins with the stereoselective addition of a new MMA molecule at the indenyl side of the zirconocene fragment. At the same time the enolate ring undergoes a stereoselective in-plane ring shift to the side opposite to the indenyl ring. These findings are used to postulate a mechanism for the polymerisation that explains the stereoselective synthesis of isotactic PMMA.

Keywords: ab initio calculations · polymerization · reaction mechanisms · zirconium

Introduction

Various zirconocene derivatives have been well established as catalysts for polymerisation of nonpolar olefins, and a large number of reports on experimental[1] and theoretical work[2] has been published in this field. However, to our knowledge, there were no theoretical studies reported on stereospecific polymerisations of methyl methacrylate (MMA) with zirconocene catalysts. As the importance of zirconocene-based polymerisations of functionalised olefins such as MMA is growing,[3] theoretical studies of the associated reaction mechanisms are expected to contribute significantly to the understanding of the selective processes. We were the first to show that [Zr{(Cp)(Ind)CMe_2}(Me)(thf)](BPh_4) (Ind = indenyl, Cp = cyclopentadienyl) is a stereoselective one-component catalyst that polymerises MMA selectively to isotactic poly(methyl methacrylate) (PMMA) with no additional cocatalysts or activators.[4] Since no theoretical investigations on stereoselective polymerisations of MMA with C_1-symmetric zirconocenes have been reported, we investigated our catalyst system by means of Hartree–Fock calculations in an effort to gain a better insight into the mechanism of the polymerisation.

The initial steps of the polymerisation of MMA were investigated by Sustmann et al. who used a model system consisting of unbridged [$Zr(Cp)_2$] fragments and acrylic acid as model substrate.[5] According to this work three different mechanisms should be possible, each of which involves a different active zirconocene species: a cationic, a neutral, and/or a bimetallic one. Since on the basis of the results of our experiments we were able to rule out the mechanisms involving bimetallic and neutral zirconocene species for our one-component catalyst system (vide infra), we considered the cationic mechanism to be active: At first MMA adds to the zirconium centre of the cationic species [Zr{$(L)_2CMe_2$}(Me)]$^+$ (L = Cp, Ind) to give [Zr{$(L)_2CMe_2$}-(Me)(MMA)]$^+$ (**1**) and then reacts with the methyl group at the zirconium centre to yield the methylated enolate **2** (Scheme 1). Then the second MMA molecule coordinates to the zirconium catalyst to yield **3**, which undergoes an intramolecular reaction with the enolate moiety already present to form **4** (Scheme 1). Hereafter, the polymerisation should proceed by repeatedly coordinating a new MMA molecule to the zirconium centre. This bound MMA molecule then reacts with the enolate moiety bound to the zirconium centre. Since our experimental work[4, 6] has shown that the single-component catalyst [Zr{(Cp)(Ind)CMe_2}(Me)(thf)](BPh_4) yields highly isotactic PMMA very efficiently, whereas syndiotactic PMMA is obtained with [Zr{$(Cp)_2CMe_2$}(Me)(thf)](BPh_4),[6] we studied the influence of the indenyl system on the reaction

[a] Prof. Dr. H. Höcker, Dr. M. Hölscher, Dr. H. Keul
Lehrstuhl für Textilchemie und Makromolekulare Chemie
der RWTH Aachen
Worringer Weg 1, 52074 Aachen (Germany)
Fax: (+49) 241-8888-185
E-mail: hoecker@dwi.rwth-aachen.de

[**] Ind = indenyl, Cp = cyclopentadienyl.

  0947-6539/01/0724-5419 $ 17.50+.50/0

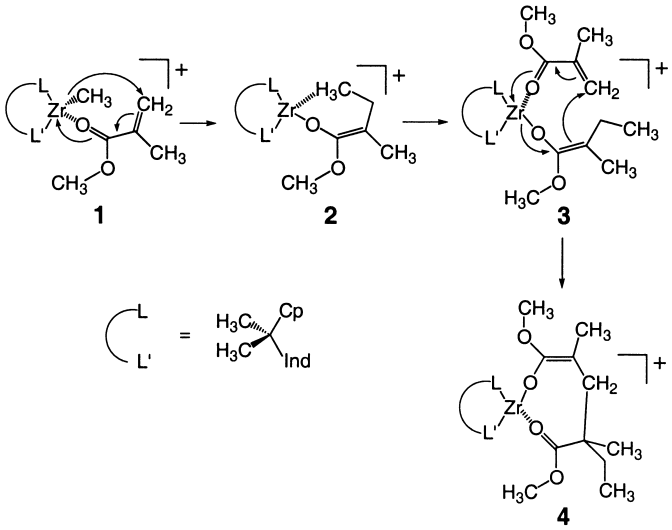

Scheme 1. Initial steps of the polymerisation of MMA with single-component cationic zirconocenes of the form $[Zr(LL')(Me)(MMA)]^+$ (in this work $LL' = (Cp)(Ind)CMe_2$).

mechanism by means of HF calculations; the results of this study are reported herein and a mechanism for the stereospecific polymerisation of MMA is postulated. We also relate this work to other studies by our group and others in which two-component systems consisting of either $[Zr\{(Cp)(Ind)CMe_2\}(Me)(thf)](BPh_4)$/$[Zr\{(Cp)(Ind)CMe_2\}(Me)(\text{-}OC(t\text{Bu})\text{=}CMe_2)]$[11] or $[Zr(Cp)_2(Me)_2]/(Ph_3C)[B(C_6F_5)_4]$[3m] were used.

Computational Details

All calculations were carried out using the Gaussian98 program package.[7] Geometry optimisations were calculated at the HF/3-21G level of theory. The 3-21G basis set gives geometries that are in good agreement with data obtained from crystal structure analyses.[8] All geometries were checked by frequency calculations to confirm that they were minima (zero imaginary frequencies) or transition states (one imaginary frequency). All geometry optimisations were carried out with no constraints or restraints, and all energies (in kcal mol^{-1}) are given as obtained and with zero-point correction (Table 1). B3LYP/Lanl2DZ and MP2(fc)/Lanl2DZ single-point energy calculations were also carried out on the HF/3-21 geometries. All metal complexes were calculated as monocations. Table 1 lists all calculated energies.

Important note: In the following text the discussion is related to the HF/3-21G energies only. But as can be seen from both Table 1 and Figures 1–5—in which the B3LYP and MP2 energy differences are given as well—the same reasoning is valid for the B3LYP and MP2 energies. A general comment on the computational methods and on the approach of the problem used in this work is made in reference [8d].

Results and Discussion

The C–C bond forming step between enolate and MMA proceeds by a redistribution of electrons between the enolate

Table 1. Energies [Hartree] of zirconocenes and MMA presented in this work. The geometries of all compounds were computed at the HF/3–21G level of theory.

Compound	HF/3–21G	HF(ZPE)/3–21G	B3LYP/Lanl2DZ	MP2(fc)/Lanl2DZ
A	–4817.0476	–4816.4965	–1356.6074	–1350.5258
B	–4817.0493	–4816.4984	–1356.6056	–1350.5290
C	–4817.0488	–4816.4982	–1356.6064	–1350.5280
D	–4817.0450	–4816.4942	–1356.6024	–1350.5252
A1	–4817.0633	–4816.5086	–1356.6146	–1350.5511
B1	–4817.0608	–4816.5097	–1356.6135	–1350.5442
C1	–4817.0622	–4816.5075	–1356.6143	–1350.5500
D1	–4817.0624	–4816.5077	–1356.6143	–1350.5488
A1-Me	–4778.2437	–4777.7207	–1317.3089	–1311.4416
A1-1	–5120.0599	–5119.4009	–1663.0329	–1655.7222
A1-2	–5120.0613	–5119.4026	–1663.0349	–1655.7238
A1-3	–5120.0776	–5119.4185	–1663.0502	–1655.7370
A1-4	–5120.0757	–5119.4163	–1663.0485	–1655.7414
B1-1	–5158.8763	–5158.1869	–1702.3386	–1694.8312
B1-2	–5158.8835	–5158.1938	–1702.3441	–1694.8354
B1-3	–5158.9004	–5158.2104	–1702.3609	–1694.8545
B1-4	–5158.8846	–5158.1927	–1702.3468	–1694.8407
C1-1	–5158.8905	–5158.2004	–1702.3509	–1694.8488
C1-2	–5158.8917	–5158.2014	–1702.3527	–1694.8502
C1-3	–5158.8965	–5158.2065	–1702.3559	–1694.8522
C1-4	–5158.8853	–5158.1956	–1702.3459	–1694.8403
D1-1	–5158.8876	–5158.1977	–1702.3489	–1694.8443
D1-2	–5158.8833	–5158.1936	–1702.3458	–1694.8417
D1-3	–5158.8956	–5158.2059	–1702.3558	–1694.8533
D1-4	–5158.8825	–5158.1927	–1702.3460	–1694.8370
A1-3-1	–5120.0959	–5119.4331	–1663.0599	–1655.7646
A1-4-1	–5120.0861	–5119.4236	–1663.0544	–1655.7587
B1-3-1	–5158.9176	–5158.2244	–1702.3693	–1694.8790
B1-4-1	–5158.9009	–5158.2078	–1702.3565	–1694.8644
TS(A1-3/A1-3-1)	–5120.0432	–5119.3842	–1663.0294	–1655.7216
TS(A1-4/A1-4-1)	–5120.0272	–5119.3676	–1663.0142	–1655.7118
TS(B1-3/B1-3-1)	–5158.8676	–5158.1779	–1702.3397	–1694.8394
TS(B1-4/B1-4-1)	–5158.8363	–5158.1460	–1702.3130	–1694.8123
MMA	–341.8056	–341.6727	–345.7292	–344.2640

0947-6539/01/0724-5420 $ 17.50+.50/0 *Chem. Eur. J.* **2001**, *7*, No. 24

and the coordinated MMA molecule (**3** → **4** in Scheme 1). During this process the nucleophilic carbon centre of the enolate unit formally reacts with the $=CH_2$ group of the MMA molecule. Therefore it is the relative orientation of the enolate and the MMA molecule that determines the configuration of the asymmetric carbon atom to be formed. Since we obtained highly isotactic PMMA, there must be stereospecific reaction channels, which are energetically and/or structurally clearly favoured over others.

Accordingly it has to be clarified first which diastereomers are obtained when MMA is added to the $[Zr\{(Cp)(Ind)CH_2\}\{\text{-O-C(OMe)=C(Me)(Et)}\}]^+$ fragment (**2** in Scheme 1). Four different complexes **A**–**D** are possible, each of which was calculated (Figure 1).

The energies of diastereomers **A**–**D** do not differ significantly, indicating that these four compounds will all be formed in the reaction (order of stability relative to **B**: **C** +0.31, **A** +1.07, **D** +2.70 kcal mol^{-1}). Thus, there is *no stereoselection* at this step and consequently all four reaction products need to be investigated. First, the structural features are explained: In **A** and **B** the enolate is located on the side opposite to the indenyl ring. Furthermore, in **A** the carbon atom C1 of the enolate resides above the O-Zr-O-plane, the carbon atom C2 of the MMA molecule below it. In the case of **B** the opposite applies. In **C** and **D** the enolate moiety is located on the same side as the indenyl ring and its C1 atom is above and below the O-Zr-O-plane, in **C** and **D**, respectively (accordingly the C2 atom of MMA is below and above the O-Zr-O-plane, in **C** and **D**, respectively). The reaction products according to Scheme 1 are compounds **A1**–**D1**, which were all calculated (Figure 1). The products **A1**, **B1**, **C1** and **D1** are lower in energy by −9.90, −7.22, −8.41, and −10.9 kcal mol^{-1} with respect to the reactants **A**, **B**, **C** and **D**, respectively. Among the four products **A1**–**D1**, it is **A1** that has the lowest energy, followed by **D1**, **C1** and **B1**, which have higher energies by +0.60, +0.70 and +1.60 kcal mol^{-1}, respectively (Figure 1). Since the energies of **A1**–**D1** lie within such a narrow range, it is reasonable to assume that *stereoselection does not take place at this step* of the reaction. Thus, the reaction channels evolving from **A1**–**D1** require investigation.

From here on we shall refer to the enolate as the enolate ring; it is the eight-membered cycle present in **A1**–**D1**, which consists of one zirconium, two oxygen and five carbon centres. One oxygen atom is an enolate oxygen atom that participates in one O–C single bond and one O–Zr single bond, the other oxygen atom is a carbonyl oxygen atom that coordinates to the zirconium centre. The bonding pattern is highlighted in Scheme 2. The whole ring is important for the stereoselectivity as will be shown.

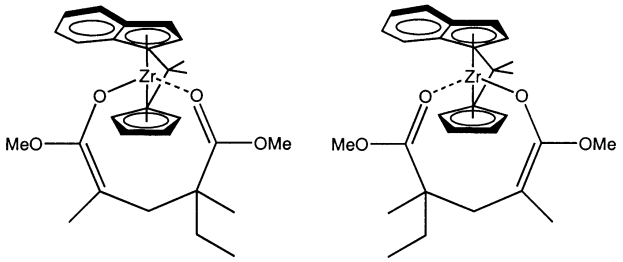

A1, B1 **C1, D1**

Scheme 2. Bonding pattern in **A1** and **B1** as well as **C1** and **D1**. Note the positions of the enolate and the C=O group.

There are two different possibilities for the next reaction step: 1) the dissociation of the coordinated O=C group from the zirconium centre of **A1**–**D1** to create a vacant coordina-

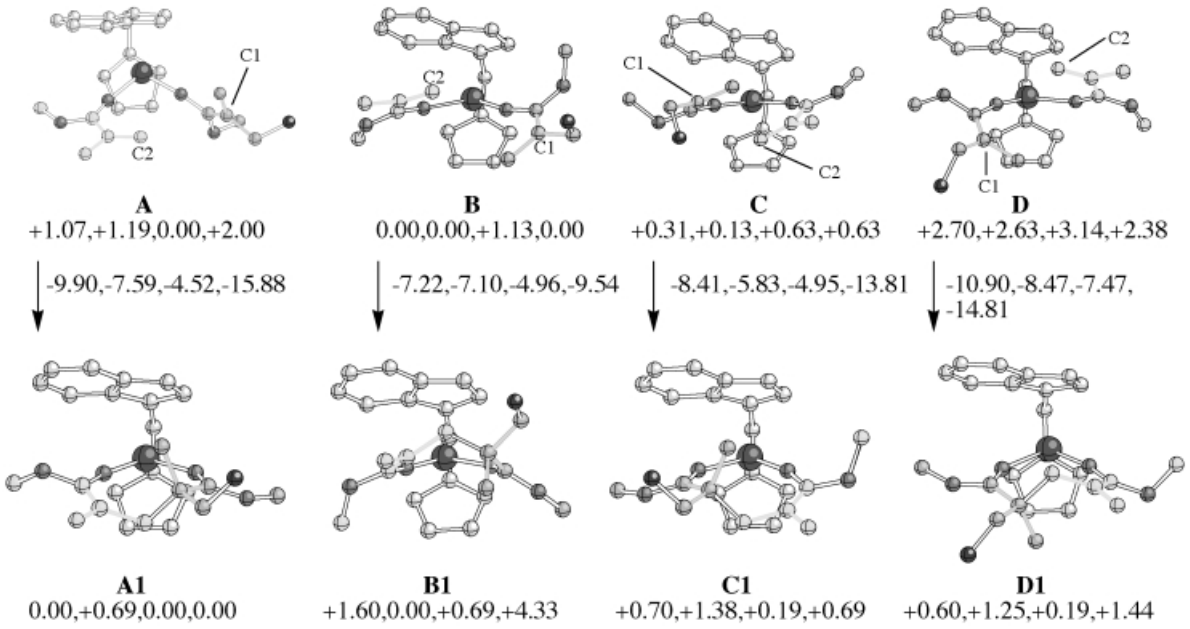

Figure 1. Calculated structures of **A**–**D** and **A1**–**D1** (the $(Cp)(Ind)CH_2$ ligand is shown in light gray and resides behind the drawing plane. Atoms in decreasing size are Zr, C, and O. Carbon atoms of MMA units are slightly darker. The carbon atom of the methyl group, which was transferred at the beginning of the reaction is dark gray. All hydrogen atoms are omitted for clarity. Energies of **A** to **D** and **B1** to **D1** are given relative to the energy of **B** and **A1**, respectively (all energies were obtained on the HF/3–21G geometries and the energy differences are given in the following order HF/3–21G, HF(zpe-corrected)/3–21G, B3LYP/Lanl2DZ, MP2(fc)/Lanl2DZ). C1 and C2 denote the reacting carbon atoms of enolate and MMA, respectively (for energies see Table 1).

tion site for the third MMA molecule or 2) the coordination of one more ligand, that is, a third MMA molecule, which would lead to a five-coordinate zirconium centre (two Cp rings, two oxygen atoms of the enolate ring and one oxygen atom of the third MMA molecule). The first possibility (dissociation of the C=O group) is energetically unfavourable as was shown before by using model complexes.[5] Furthermore, on breaking the Zr···O=C interaction the enolate moiety should be able to rotate around the $Zr-O_{enolate}$ and the $O_{enolate}-C_{enolate}$ bond which would make it even harder for a stereoselective polymerisation to take place. Therefore we began with **A1** and investigated whether it is energetically favourable for **A1** to take up one more ligand (i.e. one additional MMA molecule). It should be stressed at this point that structures of this kind, that is, a zirconium centre coordinated by two Cp rings and three oxygen atoms which are part of organic or inorganic moieties are not unusual and have been characterised by X-ray diffraction,[8] ^{91}Zr NMR spectroscopy[8b] and computational studies.[9]

How can MMA approach **A1**? It may approach from the side opposite to the indenyl ring and shift the enolate ring with the coordinated C=O group towards and partly below the indenyl ring (Figure 2; **A1-1** and **A1-2**); it also may approach from the indenyl side moving the enolate ring in the opposite direction (**A1-3** and **A1-4** in Figure 2). In both cases the coordinated MMA molecule will be oriented with its $=CH_2$ group residing either above the O-Zr-O plane of the enolate ring or below it. Thus four different diastereomers are possible, which were all calculated. Figure 2 shows the structures of the resulting products **A1-1** to **A1-4** (in these compounds the ethyl group of **A1** was replaced by a methyl group to save some computation time; to be able to compare energies the same substitution was done for **A1** and the resulting compound is designated **A1** – Me (not shown in Figure 2). The energies of **A1-1** to **A1-4** are referenced to the sum of energies of **A1** – Me + MMA). Structural details are given in Table 2.

A1-1, **A1-2**, **A1-3** and **A1-4** are calculated to be lower in energy by -6.65, -7.53, -17.76 and -16.57 kcal mol^{-1}, respectively, than the sum of the energies of the reactants. Thus, the addition of MMA to **A1** is clearly exothermic. Interestingly, it is energetically much less favourable to have the incoming MMA molecule shift the enolate ring below the indenyl system. Therefore diastereomers **A1-1** and **A1-2** are higher in energy by $+11.1$ and $+10.2$ kcal mol^{-1}, respectively, than **A1-3** which is the lowest energy diastereomer. **A1-4** is only $+1.2$ kcal mol^{-1} higher in energy than **A1-3**. These results indicate that the reaction will not involve the conformers **A1-1** and **A1-2** due to their significantly higher energies, that is, the concentrations of **A1-1** and **A1-2** in the reaction mixture can be assumed to be so profoundly low that these two compounds can be neglected for the further progress of the reaction. However, there is another fundamental reason why **A1-1** and **A1-2** will not participate further in the reaction: the $=CH_2$ group (C1 in Figure 2) of the MMA molecule in **A1-1** is much too far away to react with the enolate carbon atom (C2 in Figure 2). The MMA molecule would have to be moved towards the enolate carbon atom (C2 in Figure 2) and in this way it interferes disfavourably with the central Zr–O2 moiety, which blocks the way. The same is valid for **A1-2**.

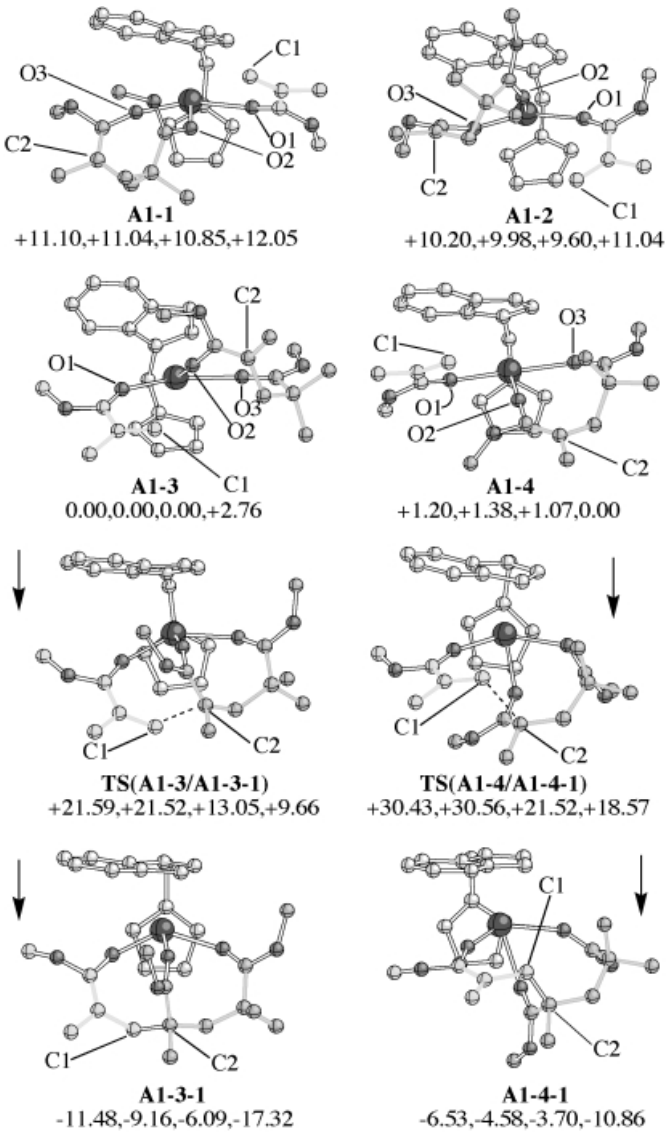

Figure 2. Calculated structures and energies of **A1-*n*** diastereomers (referenced to the energy of **A1-3**) and **A1-3-1** as well as **A1-4-1** together with the corresponding transition states **TS(A1-3/A1-3-1)** and **TS(A1-4/A1-4-1)** (energies of **A1-3-1**, **TS(A1-3/A1-3-1)** and **A1-4-1, TS(A1-4/A1-4-1)** are referenced to the energies of **A1-3** and **A1-4**, respectively; all energies were obtained on the HF/3–21G geometries and the energy differences are given in the following order HF/3–21G, HF(zpe-corrected)/3–21G, B3LYP/Lanl2DZ, MP2(fc)/Lanl2DZ; see legend to Figure 1 for atom-labelling scheme). Dotted lines between C1 and C2 in **TS(A1-3/A1-3-1)** and **TS(A1-4/A1-4-1)** denote the reacting carbon atoms of MMA and enolate, respectively. For Zr–O and C1–C2 distances see Table 2 (energies see Table 1).

A1-3 and **A1-4** are the molecules that can react directly: They have considerably lower energies than **A1-1** and **A1-2**, their reactive carbon atoms are near enough to the enolate carbon atom, and no other parts of the organic moiety or the zirconocene fragment prevent the direct approach of C1 and C2 to one another. Since the energy differences between **A1-3** and **A1-4** are negligibly low, both diastereomers *will* exist under the reaction conditions employed. Upon reaction of the

0947-6539/01/0724-5422 $ 17.50+.50/0 *Chem. Eur. J.* **2001**, *7*, No. 24

Table 2. Selected interatomic distances [Å] of **A1-*n***, **B1-n** and **D1-*n*** diastereomers as well as transition states.

Compound	Zr–O1	Zr–O2	Zr–O3	C1–C2
A1-1	2.35	2.23	1.97	6.47
A1-2	2.27	2.29	1.98	5.23
A1-3	2.30	1.98	2.33	4.15
A1-4	2.22	1.97	2.34	4.71
A1-3-1	1.99	2.30	2.28	1.58
A1-4-1	1.96	2.37	2.27	1.55
TS(A1-3/A1-3-1)	2.14	2.11	2.30	2.21
TS(A1-4/A1-4-1)	2.08	2.18	2.29	2.23
B1-1	2.30	2.27	1.97	5.28
B1-2	2.32	2.22	2.00	6.18
B1-3	2.22	1.96	2.34	3.88
B1-4	2.31	1.96	2.32	4.60
B1-3-1	1.98	2.32	2.26	1.59
B1-4-1	1.96	2.44	2.26	1.55
TS(B1-3/B1-3-1)	2.09	2.12	2.28	2.22
TS(B1-4/B1-4-1)	2.12	2.18	2.27	2.23
D1-3	2.26	1.99	2.27	6.10
D1-4	2.31	1.99	2.29	6.05

carbon atom C1 of the coordinated MMA with the carbon atom C2 of the enolate ring in **A1-3**, with the rest of the enolate ring not changing its position relative to the O-Zr-O-plane (which is not possible since all three oxygen atoms at the zirconium centre are coordinated all the time), the configuration of the newly created asymmetric carbon atom in the resulting product **A1-3-1** (C2) is *S* (it should be noted that one of the methyl groups of the former enolate ring of **A1-3** is an ethyl group in reality (Figure 2). **A1-3-1** is more stable by -11.48 kcal mol^{-1} than **A1-3**. However, if the MMA molecule is located above the O-Zr-O-plane as in **A1-4**, the configuration of the new asymmetric carbon atom in the reaction product **A1-4-1** is *R*. **A1-4-1** is more stable than **A1-4** by -6.53 kcal mol^{-1}. The activation barriers of these two reactions differ significantly (Figure 2): The energy of the transition state **TS(A1-3/A1-3-1)** is higher by $+21.59$ kcal mol^{-1} than the energy of the reactant. However, the energy of **TS(A1-4/A1-4-1)** is even higher ($+30.43$ kcal mol^{-1}) than that of the reactant and thus $+10.04$ kcal mol^{-1} higher than the energy of **TS(A1-3/A1-3-1)**. These results strongly suggest that the reaction should proceed favourably via **A1-3**.

The results of this substep are as follows: Of the four possible addition products of **A1** and MMA, there are two (**A1-1**, **A1-2**), which will not form the new C–C bond for energetic and structural reasons. Two other diastereomers (**A1-3**, **A1-4**), which are energetically and structurally much more favourable, can react. Of these two **A1-3** reacts via the energetically considerably lower transition state **TS(A1-3/A1-3-1)** (compared to the energy of **TS(A1-4/A1-4-1)**) to yield the more stable product (**A1-3-1**), and thus this reaction sequence is the one with a distinctly preferred energy profile. We consider the route via **A1-3** to **A1-3-1** to be the active reaction channel for the diastereomers following from the reaction of **A1** and MMA.

This cycle is then repeated with new MMA: Except for the growing chain the locations and orientations of the latest MMA molecule and the enolate moiety attached to the zirconium centre is the same again, meaning that all following steps start from **A1-3**- and **A1-4**-like diastereomers—with a strong preference for the reaction of **A1-3** to **A1-3-1**, as stated before. Since a detachment of the central Zr–O bond in these complexes followed by rotation of the enolate arm cannot be considered an energetically possible alternative, reactions proceeding via **A1-3** will always selectively yield *S*-configurated asymmetric carbon atoms. The postulated reaction mechanism is depicted schematically in Scheme 3.

The enolate ring of **4** is shifted by incoming MMA selectively away from the indenyl ring, and the MMA enters the coordination sphere of the zirconocene stereospecifically from the indenyl side (**5**). Thus, reactions to **5′** can be ruled out (vide infra). After C–C bond formation (**6**) either **4** is formed again or—more appropriately—the addition of new MMA with detachment of the O=C1 group of **6** proceeds simultaneously in an S_N2-type reaction (**6** → **5**). Since isotacticity

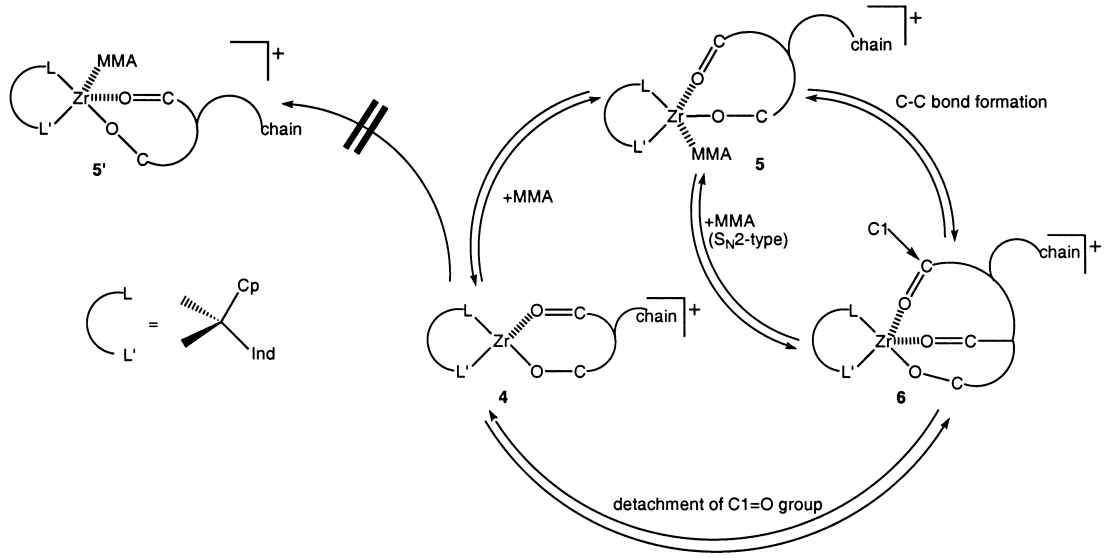

Scheme 3. Simplified reaction mechanism showing the selective shift of the enolate ring of **4** away from the indenyl ring system upon addition of MMA. An S_N2-type reaction from **6** to **5** might also be possible. Reaction to give **5′** is not favourable (see text for details).

reached very high values in our experiments, but was never 100% with $[Zr\{(Cp)(Ind)CMe_2\}(Me)]^+$ as the catalyst, it follows that the mechanism proceeds via one diastereomer (i.e. **A1-3**) for a large number of cycles and occasionally switches to the other orientation (**A1-4**-like) upon the addition of MMA (presumably due to collisions with solvent or other MMA molecules, which have enough energy to enable the more unfavourable reaction path via **A1-4**). Most probably it will also switch back again. But neither does it switch back and forth after each cycle nor does it switch very often. This also explains why we obtained higher isotacticities at low reaction temperatures (*mmmm* pentads and *mm* triads amount to 91.5 and 94.7%, respectively, at $-30\,^{\circ}C$) and lower isotacticities at higher reaction temperatures (*mmmm* pentads and *mm* diads amount to 74.9 and 84.3%, respectively, at $+30\,^{\circ}C$). This can be attributed to conformational reorientation of the enolate ring and MMA due to increased thermal motion and stronger collisions with other molecules (e.g. solvent). Actually this mechanism might also be an explanation for our results and those of others who found the $(Cp)(Flu)CMe_2$ ligand to yield an inactive catalyst:[10, 12] No matter in which direction the enolate ring moves, the resulting product is energetically not favourable.

Before considering the other diastereomers (**B1**, **C1** and **D1**), we should clarify why a two-component catalyst system consisting of $[Zr\{(Cp)(Ind)CMe_2\}(Me)(thf)](BPh_4)$ and the enolate $[Zr\{(Cp)(Ind)CMe_2\}(Me)(\text{-O-C-(O}t\text{Bu)=CMe}_2]$ polymerises MMA differently. We carried out polymerisations with different ratios of the two catalyst components and found the isotacticity (*mm* triads) to increase with a decreasing amount of enolate, while the overall yield of polymer is practically the same.[11] The enolate itself is inactive. This means that the two-component zirconocene mechanism, as was postulated by others,[3b–c, 5] is truly operative beside the single-component mechanism, but the stereoselective reaction is the result of the single-component cationic mechanism only. Thus, in our one-component catalyst system the reaction proceeds solely by the cationic mechanism outlined in Scheme 3. In the two-component catalyst system with a ratio of cationic species to enolate species >1 both the bimetallic and the cationic mechanisms are operative, but, as the experiments show, the bimetallic mechanism does not yield isotactic PMMA.

It should also be noted that unbridged zirconocene $[Zr(Cp)_2(Me)]^+$ is inactive as a catalyst for the polymerisation of MMA when BPh_4^- is the counterion,[12] whereas it is active when $MeB(C_6F_5)_3^-$[10, 12] or $B(C_6F_5)_4^-$[3m] are the counterions. These differences were investigated in detail.[13] Thus, the reaction mechanism depends on the counterion present. Consequently one has to bear in mind that the results we report here on the mechanism of the single-component system with BPh_4^- as counteranion cannot be transferred to catalyst systems with different counterions without modifications.

What would happen if MMA were added to **B1**? The corresponding diastereomers **B1-1** to **B1-4** are shown in Figure 3. They are more stable than the sum of the energies of the reactants (**B1** and MMA) by -6.21, -10.73, -21.33 and

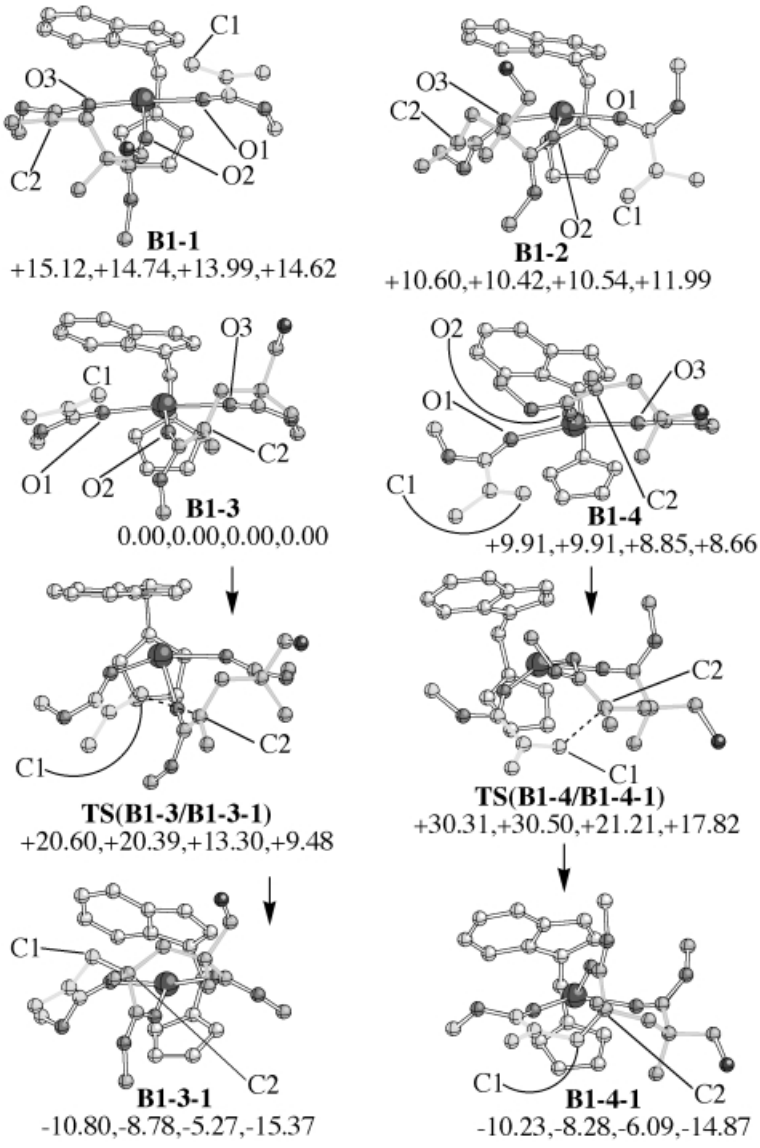

Figure 3. Calculated structures and energies of **B1-*n*** diastereomers (referenced to the energy of **B1-3**) and **B1-3-1** as well as **B1-4-1** together with the corresponding transition states **TS(B1-3/B1-3-1)** and **TS(B1-4/B1-4-1)** (energies of **B1-3-1**, **TS(B1-3/B1-3-1)** and **B1-4-1, TS(B1-4/B1-4-1)** are referenced to the energies of **B1-3** and **B1-4**, respectively; all energies were obtained on the HF/3–21G geometries and the energy differences are given in the following order HF/3–21G, HF(zpe-corrected)/3–21G, B3LYP/Lanl2DZ, MP2(fc)/Lanl2DZ; see legend to Figure 1 for atom-labelling scheme). Dotted lines between C1 and C2 in **A1-3** and **A1-4** denote the reacting carbon atoms of MMA and enolate, respectively. For Zr–O and C1–C2 distances see Table 2 (energies see Table 1).

0947-6539/01/0724-5424 $ 17.50+.50/0 *Chem. Eur. J.* **2001**, *7*, No. 24

-11.42 kcal mol^{-1}, respectively, indicating, that they are clearly exothermic products.

Again there are two complexes (**B1-1** and **B1-2**) in which the enolate ring resides below the indenyl ring. **B1-1** and **B1-2** are substantially higher in energy ($+15.12$ and $+10.60$ kcal mol^{-1}, respectively) than the lowest energy diasteromer **B1-3**. Since complexes **B1-1** and **B1-2** are so much higher in energy and show the same structural features as **A1-1** and **A1-2** (i.e. the reacting carbon atoms are too far away and the central Zr–O2 unit blocks the approach path), they are not anticipated to participate further in the reaction. In this case **B1-4** has a considerably higher energy than **B1-3** ($+9.91$ kcal mol^{-1}), which presumably prevents further reactions of **B1-4**, but we still considered it (vide infra). The two products **B1-3-1** and **B1-4-1** are -10.79 and -10.23 kcal mol^{-1}, respectively, lower in energy than the corresponding reactants. **B1-3-1** and **B1-4-1** are formed via the transition states **TS(B1-3/B1-3-1)** and **TS(B1-4/B-1-4-1)**, which are higher in energy by $+20.60$ and $+30.31$ kcal mol^{-1}, respectvely, relative to the energies of the reactants. Thus, the reaction is strongly favoured to proceed via **TS(B1-3/B1-3-1)**. This means, that starting from **B1** it is only the reaction channel proceeding via **B1-3** which is operative and **B1-4** will not be active. In this way *R*-configurated carbon atoms are produced in each new cycle.

MMA could also add to **C1** or **D1**. We shall restrict discussion to the reaction steps of **D1**, since from the discussion on **A1** and **B1** this is sufficient. However energies for **C1** and **C1-*n*** diastereomers are given in Table 1. In **D1** and in **C1** the bonding situation is reversed compared to that in **A1** and **B1**: enolate and carbonyl oxygen atoms have "exchanged" their positions (Scheme 2). The addition of MMA to **D1** leads to the formation of four different isomers **D1-1** to **D1-4** which were all optimised (Figure 4).

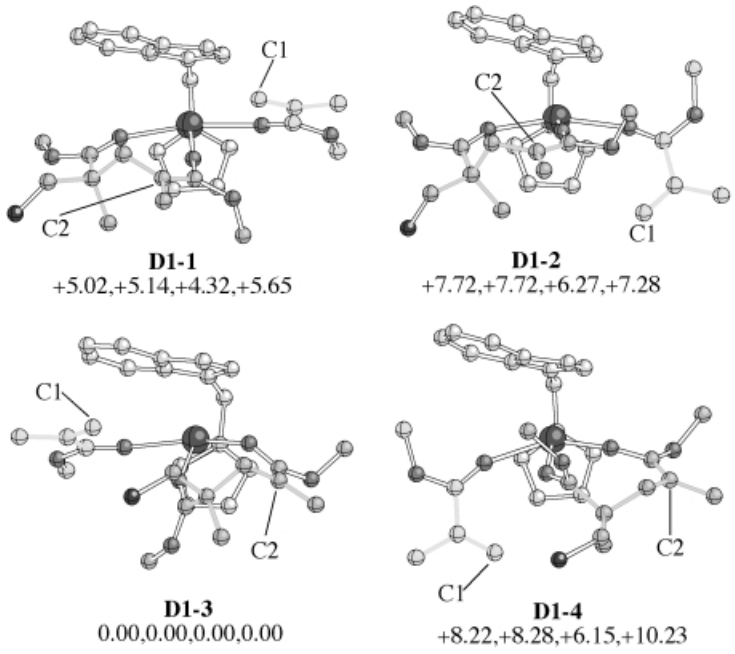

Figure 4. Calculated structures and energies of **D1-*n*** diastereomers (energies given are referenced to the energy of **D1-3**; all energies were obtained on the HF/3–21G geometries and the energy differences are given in the following order HF/3–21G, HF(zpe-corrected)/3–21G, B3LYP/Lanl2DZ, MP2(fc)/Lanl2DZ; see legend to Figure 1 for atom-labelling scheme). Zr–O distances are given in Table 2 (energies see Table 1).

Again in all four cases the addition of MMA is an exothermic process leading to energy gains of -12.3, -9.6, -17.3 and -9.1 kcal mol^{-1} for **D1-1**, **D1-2**, **D1-3** and **D1-4**, respectively (relative to the sum of the energies of **D1** and MMA). It is diastereomer **D1-3**, which is energetically clearly favoured, and again this is a compound in which the MMA resides below the indenyl system.

The C1 atom of the MMA molecule in **D1-3** now needs to react with the C2 carbon of the enolate ring, which is not only far away, but also hidden behind the O=C group coordinated to the zirconium centre. This means that with **D1-3** the same structurally based problem arises as with **A1-1** and **A1-2** (as well as **B1-1** and **B1-2**): The central Zr···O=C interaction prevents the approach of the carbon atoms to allow reaction.

As a result this reaction channel is a dead end road. However, on raising the reaction temperature (and decreasing isotacticity, vide supra) **D1-1** and **D1-2** will be present in more than negligible concentrations and thus can give rise to error pentads, since they are able to react from a structural point of view (C1 and C2 can approach each other with no hindering groups between them).

Conclusion

Polymerisation favourably proceeds via **A1-3** and **B1-3** diastereomers, in which the enolate ring has undergone an in-plane shift to the side opposite to the indenyl ring, since it is energetically clearly favourable for the enolate ring not to reside below the indenyl ring. The other **A1-*n*** and **B1-*n*** diasteromers can be ruled out energetically and/or structurally from participating in the reaction to a significant extent. Exceptions are error pentads created by **A1-4** and **B1-4** at higher temperatures. Polymerisations via **D1-3** (**C1-3**) are not possible for structural reasons (blocking units between the reacting carbon atoms), and **D1-1** and **D1-2** are energetically disfavoured (so are **C1-1** and **C1-2**; however the energy differences to **C1-3** are considerably lower, which means that **C1-1** and **C1-2** will participate more pronounced in the reaction compared to **D1-1** and **D1-2**). Thus at low reaction temperatures all **D1-*n*** diastereomers (and because of the same bonding pattern also all **C1-*n*** diastereomers) only participate to small extents, which explains the error pentads obtained. **D1-1** and **D1-2** (as well as **C1-1** and **C1-2**) whose structures permit a reaction, can play a role at higher reaction temperatures, and thus explain the decreasing isotac-

ticity. Further theoretical and experimental work is underway in this field.

Acknowledgements

This work was supported by the Bundesministerium für Forschung und Technologie (BMBF, no. 03C0276B/O). We are grateful for generous allocation of computer time by the Hochschulrechenzentrum der RWTH Aachen. We thank G. Thissen and Dr. T. Eifert for technical assistance and we are grateful for helpful discussions with Dr. T. Wagener (Marburg), Prof. Dr. G. Frenking (Marburg), and Dr. G. Raabe (Aachen).

[1] a) H.-H. Brintzinger, D. Fischer, R. Mülhaupt, B. Rieger, R. Waymouth, *Angew. Chem.* **1995**, *107*, 1255 – 1283; *Angew. Chem. Int. Ed. Engl.* **1995**, *34*, 1143 – 1164; b) G. J. P. Britovsek, V. C. Gibson, F. D. Wass, *Angew. Chem.* **1999**, *111*, 448 – 468; *Angew. Chem. Int. Ed.* **1999**, *38*, 428 – 447; c) E. Y.-X. Chen, T. J. Marks, *Chem. Rev.* **2000**, *100*, 1391 – 1434; d) L. Resconi, L. Cavallo, A. Fait, F. Piemontesi, *Chem. Rev.* **2000**, *100*, 1253 – 1345; e) G. W. Coates, *Chem. Rev.* **2000**, *100*, 1223 – 1252.

[2] a) R. Schmid, T. Ziegler, *Organometallics* **2000**, *19*, 2756 – 2765; b) L. Deng, T. Ziegler, T. K. Woo, P. Margl, L. Fan, *Organometallics* **1998**, *17*, 3240 – 3253; c) R. D. J. Froese, D. G. Musaev, K. Morokuma, *J. Mol. Struct. (Theochem)* **1999**, *461 – 462*, 121 – 135; d) M.-H. Prosenc, H.-H. Brintzinger, *Organometallics* **1997**, *16*, 3889 – 3894; e) V. L. Cruz, A. Munoz-Escalona, J. Martinez-Salazar, *Polymer* **1996**, *37*, 1663 – 1667; f) T. K. Woo, T. Ziegler, *Organometallics* **1994**, *13*, 432 – 433; g) R. Gleiter, I. Hyla-Kryspin, S. Niu, G. Erker, *Organometallics* **1993**, *12*, 3828 – 3836; h) T. K. Woo, L. Fan, T. Ziegler, *Organometallics* **1994**, *13*, 2252 – 2261; i) P. Margl, L. Deng, T. Ziegler, *Organometallics* **1998**, *17*, 933 – 946; j) P. Margl, L. Deng, T. Ziegler, *J. Am. Chem. Soc.* **1998**, *120*, 5517 – 5525; k) P. Margl, L. Deng, T. Ziegler, *J. Am. Chem. Soc.* **1999**, *121*, 154 – 162; l) A. K. Rappe, W. M. Skiff, C. J. Casewitt, *Chem. Rev.* **2000**, *100*, 1435 – 1456; m) K. Angermund, G. Fink, V. R. Jensen, R. Kleinschmidt, *Chem. Rev.* **2000**, *100*, 1457 – 1470.

[3] a) S. Collins, D. G. Ward, *J. Am. Chem. Soc.* **1992**, *114*, 5460 – 5462; b) S. Collins, D. G. Ward, K. H. Suddaby, *Macromolecules* **1994**, *27*, 7222 – 7224; c) Y. Li, D. G. Ward, S. S. Reddy, S. Collins, *Macromolecules* **1997**, *30*, 1875 – 1883; d) K. Soga, H. Deng, T. Shiono, *Macromolecules* **1994**, *27*, 7938 – 7940; e) K. Soga, H. Deng, T. Shiono, *Macromolecules* **1995**, *28*, 3067 – 3073; f) K. Soga, H. Deng, T. Shiono, *Macromol. Chem. Phys.* **1995**, *196*, 1971 – 1980; g) K. Soga, T. Saito, N. Saegusa, H. Hagihara, T. Ikeda, H. Deng, *Macromol. Chem. Phys.* **1998**, *199*, 1573; h) H. Yasuda, H. Yamamoto, K. Yokota, S. Miyake, A. Nakamura, *J. Am. Chem. Soc.* **1992**, *114*, 4908 – 4910; i) H. Yasuda, M. Furo, H. Yamamoto, S. Nakamura, N. Miyake, N. Kibino, *Macromolecules* **1992**, *25*, 5115 – 5116; j) H. Yasuda, H. Yamamoto, Y. Takemoto, M. Yamashita, K. Yokota, N. Miyake, A. Nakamuara, *Makromol. Chem. Macromol. Symp.* **1993**, *67*, 187 – 201; k) H. Yasuda, H. Yamamoto, M. Yamashita, K. Yokota, A. Nakamuara, S. Miyake, Y. Kai, N. Kanehisa, *Macromolecules* **1993**, *26*, 7134 – 7143; l) H. Yasuda, E. Ihara, *Macromol. Chem. Phys.* **1995**, *196*, 2417 – 2441; m) F. Bandermann, M. Ferenz, R. Sustmann, W. Sicking, *Macromol. Symp.* **2000**, *161*, 127 – 134.

[4] T. Stuhldreier, H. Keul, H. Höcker, *Macromol. Rapid Commun.* **2000**, *21*, 1093 – 1098.

[5] R. Sustmann, W. Sicking, F. Bandermann, M. Ferenz, *Macromolecules* **1999**, *32*, 4204 – 4213.

[6] H. Frauenrath, H. Keul, H. Höcker, *Macromolecules* **2001**, *34*, 14 – 19.

[7] Gaussian 98 (Revision A.7), M. J. Frisch, G. W. Trucks, H. B. Schlegel, G. E. Scuseria, M. A. Robb, J. R. Cheeseman, V. G. Zakrzewski, J. A. Montgomery, R. E. Stratmann, J. C. Burant, S. Dapprich, J. M. Millam, A. D. Daniels, K. N. Kudin, M. C. Strain, O. Farkas, J. Tomasi, V. Barone, M. Cossi, R. Cammi, B. Mennucci, C. Pomelli, C. Adamo, S. Clifford, J. Ochterski, G. A. Petersson, P. Y. Ayala, Q. Cui, K. Morokuma, D. K. Malick, A. D. Rabuck, K. Raghavachari, J. B. Foresman, J. Cioslowski, J. V. Ortiz, B. B. Stefanov, G. Liu, A. Liashenko, P. Piskorz, I. Komaromi, R. Gomperts, R. L. Martin, D. J. Fox, T. Keith, M. A. Al-Laham, C. Y. Peng, A. Nanayakkara, C. Gonzalez, M. Challacombe, P. M. W. Gill, B. G. Johnson, W. Chen, M. W. Wong, J. L. Andres, M. Head-Gordon, E. S. Replogle, J. A. Pople, Gaussian, Inc., Pittsburgh PA, **1998**.

[8] a) U. Thewalt, W. Lasser, *J. Organomet. Chem.* **1984**, *276*, 341 – 347; b) A. R. Siedle, R. A. Newmark, W. B. Gleason, W. M. Lamanna, *Organometallics* **1990**, *9*, 1290 – 1295; c) R. F. Jordan, C. S. Bajgur, R. Willett, B. Scott, *J. Am. Chem. Soc.* **1986**, *108*, 7410 – 7411; d) The referees pointed out to us that HF/3 – 21G energies are not state-of-the-art energies given the methods and basis sets available nowadays. We agree, and in fact HF/3 – 21G energies might be the source of misleading interpretations. However, we considered the combination of HF/3 – 21G geometries and energies appropriate because of the following cooperatively acting arguments: 1) The agreement between the calculated structures and crystal structures was considered to be good enough. 2) The ZPE-corrected HF/3 – 21G energies as well as the B3LYP/Lanl2DZ and MP2/Lanl2DZ energies on the HF/3 – 21G geometries confirmed the trends observed at the HF/3 – 21G level. 3) Treatment of the structures presented herein at a very high level and with a very large basis set will give more accurate energies, but not an unequivocal proof of the mechanism (which no calculation can). Also the possibility of obtaining new fundamental insights was contested by us and one referee. Given the computer time that would have to be spent on these structures and the presumably small gain in the understanding of the mechanism, we decided not to carry out these additional calculations at this time. 4) One referee criticised that the influence of the counterion (BPh_4^-) was not considered. This is only partly true: Carrying out calculations of this kind would be interesting, though computationally very demanding (and a combined QM/MM method would most probably be required). Chemical intuition, however, hints at not having introduced a noticeable uncertainty into this mechanism, since BPh_4^- is considered a weakly coordinating anion.

[9] a) J. W. Lauher, R. Hoffmann, *J. Am. Chem. Soc.* **1976**, *98*, 1729 – 1742; b) T. R. Ward, H.-B. Bürgi, F. Gilardoni, J. Weber, *J. Am. Chem. Soc.* **1997**, *119*, 11974 – 11985.

[10] P. A. Cameron, V. C. Gibson, A. J. Graham, *Macromolecules* **2000**, *33*, 4329 – 4335.

[11] Th. Stuhldreier, PhD Dissertation, University of Technology, Aachen (Germany) **1999**.

[12] H. Frauenrath, PhD Dissertation, University of Technology, Aachen (Germany) **2001**.

[13] X. Yang, C. L. Stern, T. J. Marks, *J. Am. Chem. Soc.* **1994**, *116*, 10015 – 10031.

Received: March 26, 2001
Revised: September 21, 2001 [F3153]

  0947-6539/01/0724-5426 $ 17.50+.50/0